

APPLICATION OF THE ADVANCED DISCRETE ELEMENT METHOD FOR THE SIMULATION OF UNSATURATED GRANULAR MATERIALS

ÁP DỤNG PHƯƠNG PHÁP PHẦN TỬ RỜI RẠC NÂNG CAO ĐỂ MÔ PHỎNG CÁC DẠNG VẬT LIỆU KHÔNG BẢO HOÀ

Thanh-Trung Vo*

Danang Architecture University

*Corresponding author: trungvt@dau.edu.vn

(Received October 19, 2020; Accepted December 20, 2020)

Abstract - By using an advanced discrete element method (DEM), the author investigates the physical and mechanical properties of unsaturated granular materials via the diametrical compression test of wet aggregates, the impact of wet aggregates on a rigid plane, and the collapse of an unsaturated granular column. The advanced discrete element method is characterized by the classical DEM with the capillary cohesion law enhanced by the cohesive and viscous forces between particles. The paper shows that the aggregates are ductile and no abrupt rupture due to the rearrangement of primary particles and the tensile effects of the cohesive forces having the direction perpendicular to the impact direction, the mechanical strength of aggregates depends on the liquid properties and the impact speed, and the collapse of the wet granular column strongly depends on the natural properties of the liquid. These results are consistent and thus providing the potential application of the advanced DEM in unsaturated granular media.

Key words - Discrete Element Method (DEM); mechanical strength; collapse; capillary bridge

1. Introduction

The Discrete Element Method (DEM) has been extensively used for the simulations of the physical and mechanical properties of granular materials for the last few decades [1, 2]. This numerical approach is based on the step-wise integration of the equations of motion for all particles/grains by taking into account the particle interactions [3]. The particle interactions are characterized by the elastic and frictional forces. In unsaturated granular materials, however, the interactions between particles not only involve the elastic and frictional forces but also the liquid forces due to the presence of the interstitial liquid inside granular media [4, 5].

In advanced DEM, it is possible to implement the interstitial liquid inside dry granular materials by considering the cohesive and viscous forces of such liquid [4-7]. In unsaturated granular materials, the capillary cohesive forces and viscous forces are induced in capillary bridges between wet grains. The capillary bridges are formed as a consequence of the mixing dry particles with the liquid, the infiltration of the rainwater into soils, or condensation of the liquid-vapor inside granular media. These capillary bridges may be broken or reformed during the movements of granular particles as a consequence of colliding with other particles or walls. These physical assumptions are clearly appropriate with the environment of unsaturated granular materials.

In this paper, the author presents the numerical investigations of the physical and mechanical properties of

Tóm tắt - Bài báo khảo sát một số đặc tính vật lý và cơ học của vật liệu không bão hoà thông qua mô hình nén khối kết tụ tròn hay sự va chạm của nó trên một mặt phẳng cứng, và sự sụp đổ của cột vật liệu ướt bằng cách sử dụng phương pháp phần tử rời rạc nâng cao. Phương pháp này được phát triển từ phương pháp phần tử rời rạc cổ điển kết hợp với quy luật kết dính của các mao mạch, đặc trưng bởi lực dính và lực nhớt. Bài báo thể hiện các khối kết tụ ướt là mềm dẻo và không bị phá huỷ tức thời do việc sắp xếp lại các hạt bên trong và do ảnh hưởng của lực kéo có phương vuông góc với phương tác dụng lực. Sự sụp đổ của các cột vật liệu ướt phụ thuộc vào các đặc tính tự nhiên của chất lỏng. Những kết quả này là hợp lý và do vậy bài báo thể hiện khả năng áp dụng tiềm tàng của phương pháp phần tử rời rạc nâng cao trong môi trường vật liệu không bão hoà.

Từ khóa - Phương pháp phần tử rời rạc (DEM); cường độ; sự sụp đổ; cầu mao dẫn

unsaturated granular materials via the diametrical compression test and the impact test of wet aggregates as well as the collapse of unsaturated granular column by varying different values of the interstitial liquid. As we shall see the results of these tests are consistent and thus illustrate the potential applications of the advanced DEM in wet granular materials.

2. Advanced discrete element method

In this current work, the simulations are modeled by using the cFGd-3D++ code that has been developed for simulating the granular materials. The code is based on the platform of the advanced discrete element method with the availability of the solid-liquid interactions. In advanced DEM, the equation of motion of particle i with the radius R_i is governed by the Newton's second law [2]:

$$m_i \frac{d^2 \mathbf{r}_i}{dt^2} = \sum_j [(f_n^{ij} + f_c^{ij} + f_v^{ij}) \mathbf{n}^{ij} + f_t^{ij} \mathbf{t}^{ij}] + m_i \mathbf{g} \quad (1)$$

Where, m_i and \mathbf{r}_i are the mass and position vector of particle i . Particle j is the neighboring of particle i . \mathbf{g} is the gravitational acceleration vector. \mathbf{n}^{ij} and \mathbf{t}^{ij} are the unit vectors that perpendicular and in the contact plane between two particles in contact, respectively. f_n is the normal contact force between two spherical particles. f_c and f_v are the normal capillary cohesion force and normal viscous force, and f_t denotes the tangential force.

The normal contact force $f_n = f_n^d + f_n^e$, where $f_n^d = \gamma_n \delta_n$ is the normal damping force, proportional to the

relative normal velocity δ_n , where γ_n is the normal damping parameter. $f_n^e = k_n \delta_n$ is the normal elastic force, proportional to the gap δ_n and the normal stiffness k_n . The tangential force f_t is the minimum of the summarize of the tangential elastic force $f_t^e = k_t \delta_t$ and the tangential damping force $f_t^d = \gamma_t \delta_t$ and the force threshold μf_n according to the Coulomb friction law, where k_t and γ_t are the tangential stiffness and the tangential damping parameter. δ_t and δ_n are the relative tangential displacement and the relative tangential velocity between particle i and j [8].

The capillary cohesion force f_c between two grains depends on the volume of the capillary bond V_b , the liquid-vapor surface tension γ_s , and the solid-liquid contact angle Θ . The cohesion force is given by the following expression [5, 9]:

$$f_c = \begin{cases} -\xi R \text{ for } \delta_n \leq 0 \\ -\xi R e^{-\frac{\delta_n}{\lambda}} \text{ for } 0 < \delta_n \leq d_{rupt} \\ 0 \text{ for } \delta_n > d_{rupt} \end{cases} \quad (2)$$

Where, $\xi = 2\pi\gamma_s \cos\Theta$ is the pre-factor of the capillary cohesion force. $R = \sqrt{R_i R_j}$ is the mean radius of two particle i and j in contact. λ is the characteristic length, considering the fall off of the capillary cohesion force when the gap tend to increase. d_{rupt} is the debonding distance, is given by the following expression:

$$d_{rupt} = \left(1 + \frac{\Theta}{2}\right)^{1/2} \quad (3)$$

The normal viscous force is due to the lubrication effects of the binding liquid, is given by [10]:

$$f_v = \begin{cases} \frac{3}{2} \pi R^2 \eta \frac{v_n}{\delta_0} \text{ for } \delta_n \leq 0 \\ \frac{3}{2} \pi R^2 \eta \frac{v_n}{\delta_n + \delta_0} \text{ for } 0 < \delta_n \leq d_{rupt} \\ 0 \text{ for } \delta_n > d_{rupt} \end{cases} \quad (4)$$

where η denotes the liquid viscosity, v_n and δ_0 are the relative normal velocity and the characteristic length of the particle roughness. All the simulation parameters used in this paper are shown in Table 1.

Table 1. Simulation parameters

Parameter	Symbol	Value	Unit
Particle density	ρ	2600	$kg \cdot m^{-3}$
Coefficient of friction	μ	0.4	
Normal stiffness	k_n	10^6	N/m
Tangential stiffness	k_t	$8 \cdot 10^5$	N/m
Normal damping	γ_n	0.5	Ns/m
Tangential damping	γ_t	0.5	Ns/m
Viscosity of liquid	η	1.0	mPa.s
Time step	Δt	$8 \cdot 10^{-8}$	s

3. Results

3.1. Mechanical properties of aggregates

The aggregates composed wet primary particles are an important operation not only in the nature such as clumps of soils but also in industry such as iron ore production. The mechanical properties of aggregates reflect the stiffness of such aggregates under the action of the collision forces such

as compression and the impact with rigid plane. Upon the collision, the aggregates change its strength due to the relative displacements of primary particles and the interactions between them. However, the evolution speed and the peak of the mechanical strength depend on the impact method and the material properties of wet aggregates. The mechanical strength of wet particle aggregates is characterized by the average vertical stress that obtained from the simulations by considering the total normal forces and the branch vector which joining the particle centers.

$$\sigma_{zz} = \frac{1}{V} \sum_{k=1}^N f_z^k l_z^k = n_b \langle f_z^k l_z^k \rangle \quad (5)$$

Where, V is the volume of aggregate, N is the number of capillary bridges between particles in the calculational step, n_b denotes the number density of the capillary bridges, f_z and l_z are the z-components of the normal forces and the branch vector.

3.1.1. Diametrical compression test

Figure 1 shows the model of the diametrical compression test of a single aggregate and the force chains distribution of the normal forces at the beginning of the compression process. The bottom wall is fixed and the top wall is applied by a constant downward velocity. At the beginning of the compression test, some primary particles are in contact with the top and bottom walls. The number of primary particles contacting with the walls increases due to the deformation of the aggregates. However, the aggregates do not break into different parts due to the effects of the debonding distance of the capillary bridges.

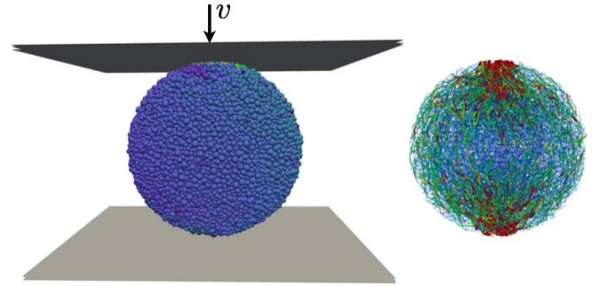


Figure 1. Schematic representation of the diametrical compression test of wet particle aggregate (left) and force chains distribution inside aggregate (right). The line thickness corresponds to the magnitude of the normal forces

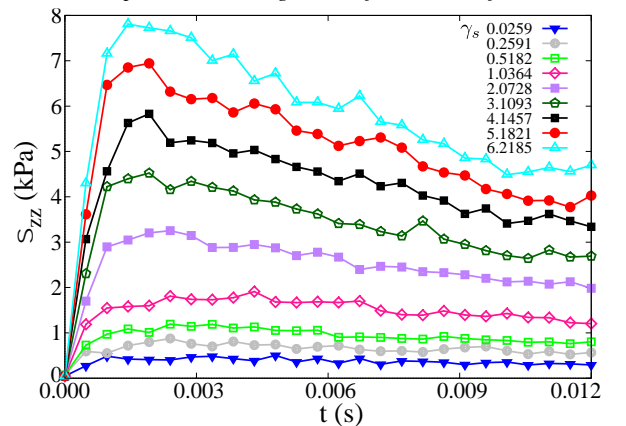


Figure 2. Evolution of the vertical stress of wet aggregate as a function of the compression time for different values of the liquid-vapor surface tension

Figure 2 displays the evolution of the mean vertical stress σ_{zz} as a function of the compression time for different values of the liquid-vapor surface tension of the liquid. As we can see, the aggregate strength first increases rapidly and reaches a plateau. Then, this strength declines smoothly due to breaking of the capillary bridges. The plateau of the vertical stress represents the ductile behavior of wet aggregates due to the rearrangement of primary particles as well as the tensile effects of the cohesive forces having the direction perpendicular to the compression direction. These mechanical responses of wet aggregates are consistent with previous investigation in experiment.

3.1.2. Vertical impact test

Similarly, the mechanical response of wet aggregates is also investigated by generating the impact test of a single wet aggregate on a flat plane. Figure 3 represents the numerical model of the aggregate impacting on a rigid plane and the force chains distribution at the early-stage impact of such aggregate. In this simulation, the aggregate was set at its initial height that equals to a half of its radius, measured from the lowest point of aggregate to the rigid plane. Then, the aggregate starts flowing down to collide with the plane by setting an initial velocity and activating the particle gravity.

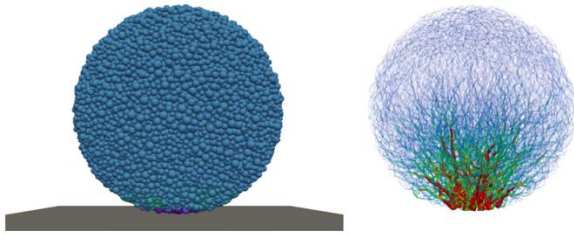


Figure 3. Schematic representation of the impact test of a single wet aggregate on a flat plane (left) and force chains distribution inside aggregate (right). The lines thickness and their colors represent the magnitude of the normal force

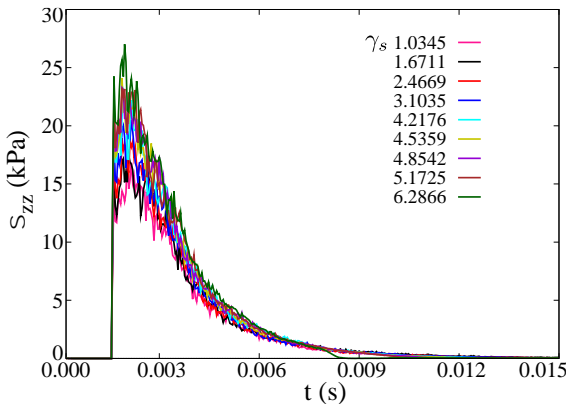


Figure 4. Evolution of the mean vertical stress of a single wet aggregate impacting on a rigid plane as a function of the impact time for different values of the liquid-vapor surface tension

Figure 4 displays the evolution of the mean vertical stress as a function of the impact time for different values of the surface tension of the capillary bonds between spherical particles. In this test, the aggregate strength equal zero before occurring the collision with the rigid plane corresponding to the stability of the aggregate. Then, the mean vertical stress suddenly jumps at the early-stage

impact and reaches a plateau before the onset failure of the aggregates due to losing the capillary bonds. Similar to the diametrical compression test, the aggregates do not break into different parts due to the particle rearrangements and tensile effects of the capillary bonds.

3.2. Collapse of wet granular column

Beside investigation the mechanical response of unsaturated granular materials such as diametrical compression and impact tests above, it is interesting to consider here the potential application of the advanced DEM in landslides, slope failure, and granular collapse. In this paper, the author investigates the collapse dynamics of unsaturated granular column when considering both effects of the cohesive and viscous forces of the capillary bonds. The granular column is considered with a periodic boundary condition through the lateral axis which perpendicular to the flow direction of granular materials.

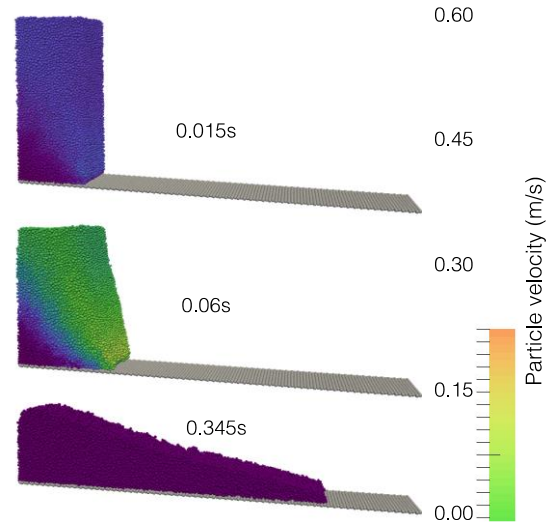


Figure 5. Snapshots represent the collapse of an unsaturated granular column on a rough wall. The particles color represents their velocities during the collapse

Figure 5 displays the time sequence of the collapse of a granular column on a rough wall by gluing mono-spheres. The granular column is first prepared by using an isotropic compaction in a rectangular. Then, the author activates the particle density as well as the cohesive and viscous forces of the binding liquid. After that, we removed the walls and replaced by the periodic boundary conditions along the y-direction of the model. The bottom rough wall is fixed, and system is free on the top. Almost particles start falling vertically with the velocity that increases due to the effects of the particle gravity. After a period of delay, the particles start flowing forward with a toe of granular column. During these stages, the kinetic energy of particle changes from vertical direction to horizontal one. This change is more less fast depending on the natural properties of the liquid.

Figure 6 shows the evolution of the normalized kinetic energy in the vertical $E_{cz} = \frac{1}{2} \sum_{k=1}^{N_p} m_k v_{kz}^2$ and horizontal $E_{cx} = \frac{1}{2} \sum_{k=1}^{N_p} m_k v_{kx}^2$ directions by potential energy $E_p = \sum_{k=1}^{N_p} m_k g h_k$ of the granular column for different values of the liquid-vapor surface tension of the capillary

bonds, where N_p is the number of particles, v_{kx} and v_{kz} are the x and z components of the k particle velocity, respectively. m_k is the mass of particle k , h_k denotes the height of particle k as compared to the rough wall position. As we can see, the particle energy first increases rapidly in the vertical direction and reaches the peak before declines rapidly as a consequence of the transition from vertical kinetic energy to horizontal kinetic energy as well as the dissipation of the particle energy during the movements. Then, the particles reach the final-stage deposition more less fast depending on the parameters. These physical properties are also consistent with previous investigations in both simulations and experiments.

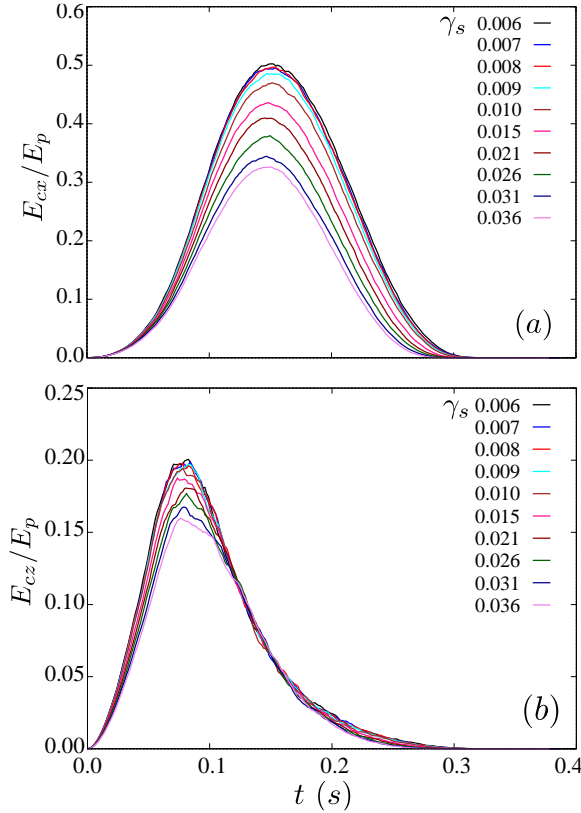


Figure 6. Evolution of the horizontal kinetic energy E_{cx} (a) and the vertical kinetic energy E_{cz} (b) normalized by the potential energy E_p as a function of the collapse time for different values of the liquid-vapor surface tension

4. Computational aspects

Based on the examples above, we can see that the main advantages of the advanced DEM are simple and easily investigate the physical and mechanical properties of granular materials due to easily access the particle scale and vary broad range of values of the parameters. However, due to the implementation of the interstitial liquid inside granular materials, the computation of the particle interactions requires much more computational power and memory in

order to discretize the degrees of the freedom associated with the liquid phase. For this reason, it is essential to generate a suitable model which considering the balance between the computational efficiency and the physical and mechanical realisms of granular materials.

In order to deal with the problem above, however, the parallel implementation is one of the main solution which not only help to increase the number of particles in the model (physical and mechanical realisms) but also help to decrease the computational time. The speed of the computational process will be increased proportional to the number of the processors. Thus, the parallel performance of the author code (cFGd3D-c++ code) is the first priority for the applications of the advanced DEM in unsaturated granular materials.

5. Conclusions

In this paper, the author used an extensive 3D discrete element method for the simulation three different cases of unsaturated granular materials. The current paper shows that the aggregates are ductile and no abrupt rupture due to representation the rearrangement of primary particles as well as the tensile effects of the capillary bonds, and the mechanical strength of wet aggregates strongly depends on the material properties such as the liquid-vapor surface tension. The collapse of granular column on a rough wall also represents the appropriate physical responses of granular materials. These physical and mechanical responses of unsaturated granular materials are consistent and thus providing a potential application of the advanced DEM for the simulation of granular media.

REFERENCES

- [1] P. A. Cundall O. D. L. Strack, "A discrete numerical model for granular assemblies", *Géotechnique* 29 (1), 1979 47-65.
- [2] F. Radjai, F. Dubois, "Discrete-element modeling of granular materials", Wiley-Iste, 2011.
- [3] S. Luding, "Collisions and contacts between two particles, in Physics of Dry granular media", *NATO ASI Series E350*, edited by H. J. Hermann, J.-P. Hovi, and S. Luding, 1998 285.
- [4] T.-T. Vo, S. Nezamabadi, P. Mutabaruka, J.-Y. Delenne, and F. Radjai, "Additive rheology of complex granular flows", *Nature Communications* 11, 1476, 2020.
- [5] T.-T. Vo, "*Erosion dynamics of wet particle agglomerates*", *Comput. Part. Mech.*, 2020.
- [6] T.-T. Vo, P. Mutabaruka, S. Nezamabadi, J.-Y. Delenne, E. Izard, R. Pellenq, F. Radjai, "Mechanical strength of wet particle agglomerates", *Mech. Res. Commun.* 92, 1, 2018.
- [7] T.-T. Vo, "Rheology and granular texture of viscoinertial simple shear flows", *J. Rheol.* 64, 1133, 2020.
- [8] S. Dippel, G. G. Batrouni, D. E. Wolf, "How transversal fluctuations affect the friction of a particle on a rough incline", *Phys. Rev. E* 56, 3645, 1997.
- [9] C. Willett, M. Adans, S. Johnson, J. Seville, "Capillary bridges between two spherical bodies", *Langmuir* 16, 9396, 2000.
- [10] G. Lefebvre, P. Jop, "Erosion dynamics of a wet granular medium", *Phys. E* 8, 032205, 2013.